Influences of Variation in Geometry of Tape Insert on Thermal Performance and Flow Characteristics in Tubes

[Taiwo O. Oni and Manosh C. Paul]

Abstract—**This paper presents the results of the numerical investigation carried out on different tube designs to assess the impacts of variations in the geometry of the twisted tape on heat transfer, friction factor and thermal performance of water inside the tubes. Alternate-axis triangular cut twisted tape was considered and its pitch and width, as well as the perimeter of the cuts on it were varied. The walls of the tubes were subjected to a uniform heat flux condition. The results of the investigation revealed that the thermal performance of the tube designs improved with an increase in the width of the tape and an increase in the size of the cuts on the tape but diminished as the pitch of the tape increases.**

Keywords—**Twisted tape, heat transfer, thermal performance, designs**

I. Introduction

Due to the ease of installation, low cost and low maintenance, the use of twisted tape inserts has become a reliable technique for promotion of heat transfer [1, 2]. These techniques have found various applications in the process industries (air-cooled finned tube heat exchangers), automobile industries (radiators and internal heat exchangers) and residences (radiators, refrigeration systems and condensing central heating exchangers) [3-5]. The twisted tape generates a swirl flow which induces turbulence near the wall of the tube. This increase in the turbulent intensity near the tube improves fluid mixing in the tube and eventually leads to enhancement of heat transfer [2-6].

Some researchers have investigated the roles played by twisted tape in its application in heat transfer and they have made it known that the shapes of cuts made on the tape to modify them (the tape) has effects on the heat transfer promotion. Murugesan et al. [7] produced a trapezoidal-cut twisted-tape insert and later [8] fabricated a twisted-tape insert with square cuts. Chiu and Jang [9] reported on a

longitudinal strip insert with holes, Cui and Tian [10] fabricated an edge-fold twisted tape and Chang et al. [11] formulated a serrated twisted tape. These researchers as well as the findings from the other works indicated that the heat transfer produced by tubes induced with these modified twisted tapes is higher than those produced in the tubes without a twisted tape.

The present work is carrying out simulation on different tube designs with twisted tape having different geometries in their pitch, width and size of cuts made on them. The aim is to examine the effects which the variations of these geometries have on the heat transfer in the tubes.

II. Geometry of Flow Models

Seven different flow models are considered in this study. Each of them consists of a tube induced with a twisted tape. The tube is 1000mm long and 19mm in diameter and the tape runs through the entire length of the tube. Each of the tapes has alternate axes and equilateral triangular cuts on them. The tape in each of the flow models is different from one another in width (w), pitch (y), length of a side of the triangular cut (s) and perimeter of cut (p) as demonstrated in Fig. 1 and Table I. The tapes are named as alternate-axis triangular cut twisted tape (ATCT) while the flow models are referred to as tube with alternate-axis triangular cut twisted tape (TATCT).

III. Mathematical Formulation

The flow is assumed to be steady, and incompressible Newtonian and they are governed by the three-dimensional Navier-Stokes equations [12]. Turbulent flow is considered and the appropriate models are applied to determine the unknown variables in the RANS (Reynolds Averaged Navier-Stokes) equations as discussed below.

A. Navier-Stokes Equations

The Navier-Stokes equations [21, 22] are given as

(a)   Continuity equation:

$$\nabla . \boldsymbol{V} = 0 \tag{1}$$

(b)   Momentum equation:

$$\rho \, \frac{\partial \boldsymbol{V}}{\partial t} + \nabla . (\rho \boldsymbol{V}\boldsymbol{V}) = -\nabla P + \nabla . \mu(\nabla \boldsymbol{V}) \tag{2}$$

Taiwo O. Oni* and Manosh C. Paul**

Systems, Power & Energy Research Division, School of Engineering
University of Glasgow, Glasgow G12 8QQ, UK
E-mail: * t.oni.1@research.gla.ac.uk; tooni1610@yahoo.com
         **Manosh.Paul@glasgow.ac.uk

(c) Energy equation:

$$\rho C_p \left(\frac{\partial T}{\partial t} + \nabla.\mathbf{V}T \right) = \nabla.(k.\nabla T) \tag{3}$$
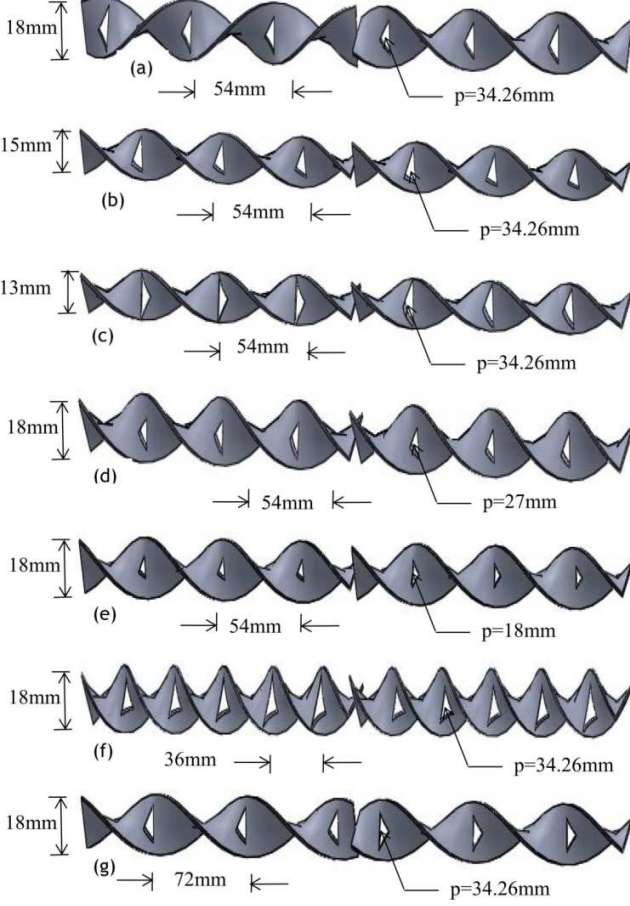

Figure 1. Geometries of the alternate-axis triangular cut twisted tape of (a) TATCT, (b) TATCTw1, (c) TATCTw2, (d) TATCTa1, (e) TATCTa2, (f) TATCTy1 and (g) TATCTy2.

TABLE I. DESCRIPTION OF THE VARIOUS GEOMETRIES OF THE ALTERNATE-AXIS TRIANGULAR CUT TWISTED TAPE (ATCT) USED FOR THE DOMAINS OF THE TATCT

Tape	Geometry			
	w (mm)	y (mm)	s(mm)	p (mm)
ATCT	18	54	11.42	34.26
ATCTw1	15	54	11.42	34.26
ATCTw2	13	54	11.42	34.26
ATCTa1	18	54	9.00	27.00
ATCTa2	18	54	6.00	18.00
ATCTy1	18	36	11.42	34.26
ATCTy2	18	72	11.42	34.26

where T is the temperature, μ is the dynamic viscosity, P is the pressure, k is the thermal conductivity, ρ is the density and C_p is the heat capacity at constant pressure.

B. RANS Equations

The RANS equations [13, 14] are written as

(a) Mass conservation:

$$\frac{\partial}{\partial x_i}(u_i) = 0 \tag{4}$$

(b) Momentum equation:

$$\rho \frac{D\overline{u_i}}{Dt} = S_i - \frac{\partial \overline{P}}{\partial x_i} + \frac{\partial}{\partial x_j}\left(\mu \frac{\partial u_i}{\partial x_j} - \rho \overline{u_i' u_j'} \right) \tag{5}$$

(c) Time-averaged energy equation:

$$\frac{\partial}{\partial x_j} \rho C_p (u_j T) = u_j \frac{\partial P}{\partial x_j}$$
$$+ u_j' \frac{\partial P'}{\partial x_j} + \frac{\partial}{\partial x_j}\left(k \frac{\partial T}{\partial x_j} - \rho C_p \overline{u_j' T'} \right) \tag{6}$$

IV. Turbulence Modelling

The turbulence models used for the simulation are discussed below.

A. Standard $\kappa - \varepsilon$ Model

The standard $\kappa - \varepsilon$ model [15] is based on turbulent kinetic energy (κ) and dissipation rate of turbulence kinetic energy (ε). The transport equations [14] are given as:

$$\frac{\partial}{\partial t}(\rho\kappa) + \frac{\partial}{\partial x_i}(\rho\kappa u_i) = \frac{\partial}{\partial x_j}\left[\left(\mu + \frac{\mu_t}{\sigma_\kappa}\right)\frac{\partial\kappa}{\partial x_j}\right]$$
$$+ G_k - \rho\varepsilon - Y_M + S_k \tag{7}$$

$$\frac{\partial}{\partial t}(\rho\varepsilon) + \frac{\partial}{\partial x_i}(\rho\varepsilon u_i) = \frac{\partial}{\partial x_j}\left[\left(\mu + \frac{\mu_t}{\sigma_\varepsilon}\right)\frac{\partial\varepsilon}{\partial x_j}\right]$$
$$+ C_{1\varepsilon}\frac{\varepsilon}{\kappa}G_k - C_{2\varepsilon}\rho\frac{\varepsilon^2}{\kappa} + S_\varepsilon \tag{8}$$

The turbulent viscosity (μ_t) is modelled as

$$\mu_t = \rho C_\mu \frac{\kappa^2}{\varepsilon} \tag{9}$$

where G_κ is the generation of κ due to the mean velocity gradients; $C_{1\varepsilon}, C_{2\varepsilon}, C_{3\varepsilon}$ are model constants; σ_κ and σ_ε are the turbulent Prandtl numbers for κ and ε respectively; S_k and S_ε are user-defined source terms. The model constant are $C_{1\varepsilon} = 1.44, C_{2\varepsilon} = 1.92, C_\mu = 0.09, \sigma_\kappa = 1.0, \sigma_\varepsilon = 1.3$ [14].

B. RNG $\kappa - \varepsilon$ Model

The Renormalization Group theory (RNG) κ-ε model [16] has model transport equations for κ and ε. Its transport equations [14] are

$$\frac{\partial}{\partial t}(\rho\kappa) + \frac{\partial}{\partial x_i}(\rho\kappa u_i) = \frac{\partial}{\partial x_j}\left[\alpha_\kappa\mu_{eff}\,\frac{\partial\kappa}{\partial x_j}\right]$$
$$+G_k + G_b - \rho\varepsilon - Y_M + S_k \tag{10}$$

$$\frac{\partial}{\partial t}(\rho\varepsilon) + \frac{\partial}{\partial x_i} = \frac{\partial}{\partial x_j}\left[\alpha_\epsilon\mu_{eff}\,\frac{\partial\varepsilon}{\partial x_j}\right]$$
$$+ C_{1\varepsilon}\frac{\varepsilon}{\kappa}(G_k + C_{3\varepsilon}G_b) - C_{2\varepsilon}\,\rho\,\frac{\varepsilon^2}{\kappa} - R_\varepsilon + S_\varepsilon \tag{11}$$

where α_κ and α_ϵ are the inverse effective Prandtl numbers for κ and ε respectively; $C_{1\varepsilon} = 1.42$, $C_{2\varepsilon} = 1.68$, $C_\mu = 0.0845$, $\sigma_\kappa = 0.7194$ and $\sigma_\varepsilon = 0.7194$ are model constants [14].

V. Boundary Conditions

Turbulent flow with Reynolds number between 5000 and 20000 were considered. A uniform heat flux condition is applied to the surface of tube wall and it is subjected to a no slip condition, i.e. $u_i = u_j = u_k = 0$.. A velocity and temperature of $301K$ are specified at the inlet of the tube. The turbulence intensity, I is given by the expression in equation (14). At the outlet, the gauge pressure is set to zero, a backflow temperature is specified.

$$I = 0.16Re^{-0.125} \tag{12}$$

where Re = Reynolds number and D = tube diameter.

VI. Numerical Technique

The governing partial differential equations mentioned above are solved by finite volume method. The calculation of pressure and velocity [13] was coupled by the Semi Implicit Pressure Linked Equations (SIMPLE) algorithm. Fluent [14] was used to obtain the iterative solution of the equations. Grid independence tests were conducted on the domains. As provided in Table II, the domains TATCT, TATCT_{w1}, TATCT_{w2}, TATCT_{a1}, TATCT_{a2}, TATCT_{y1}, TATCT_{y2} become grid independent at cells 2515756,

TABLE II. Grid independence test for various domains of TATCT

Domain	Cell		
TATCT	1658638	2515756	3018907
TATCTw1	947018	1042326	1904321
TATCTw2	810424	939615	1045580
TATCTa1	944241	1154115	1301128
TATCTa2	879649	1038263	1271045
TATCTy1	1002701	1247268	1381714
TATCTy2	1106413	1349955	1484286

1042326, 939615, 1154115, 1038263, 1247268 and 1349955 respectively.

VII. Results and discussions

The computational results are discussed in this section.

A. Contour of Temperature

The temperature contour for the different tube designs can be found in Fig. 2. Frames (a), (b) and (c) show the tubes with tape width w = 18mm, 15mm and 13mm respectively. The tube with w = 18mm provide better temperature distribution than that with w=15mm and 13 mm. This is as a result of more efficient mixing inside the domain. As the perimeter (p) of the cut is reduced from 43.26mm (frame a) to 27mm (frame d) and 18mm (frame e), the thermal boundary layer grows thinner and the temperature distribution is affected. When the pitch (y) is reduced from 54mm (frame a) to 36 mm (frame f), the temperature distribution improves but reverse is the case when it is increased to 72mm (frame g).
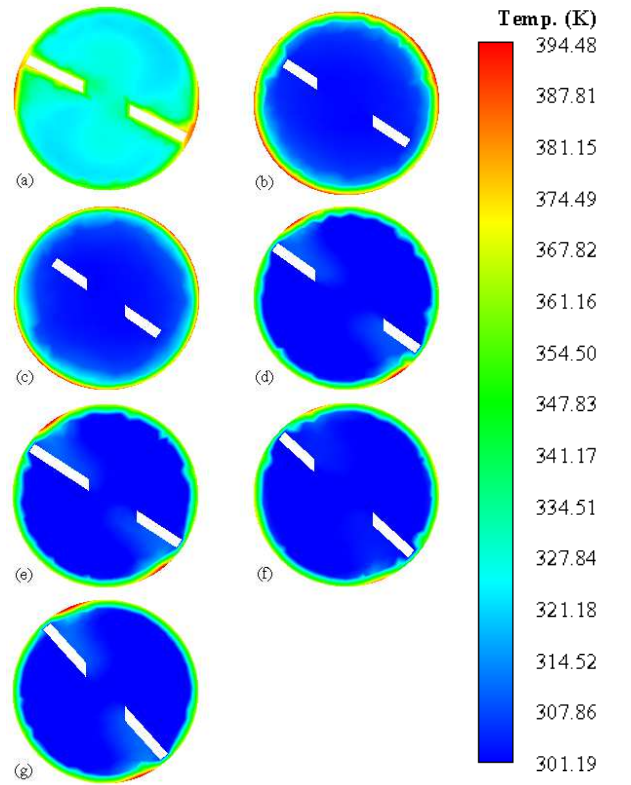

Figure 2. Contour plots of static temperature (K) for the domains of (a) TATCT, (b) TATCT_{w1}, (c) TATCT_{w2}, (d) TATCT_{a1}, (e) TATCT_{a2}, (f) TATCT_{y1} and (g) TATCT_{y2} for Re =20000.

B. Impacts of the Variations in the Tape Geometries on Heat Transfer

The heat transfer is expressed in term of Nusselt number. The effects of the variations in the geometries of the tape on the heat transfer are presented Fig. 3. The heat transfer decreases with decreasing width. This is because the domain with the largest free space ($TATCT_{w2}$) between the tube wall and edge of the tape generates the weakest swirl flow, but the domain with the highest tape width (TATCT) creates the strongest swirl, resulting in effective transfer of heat across the layers of the fluids. The Nusselt number with tape geometry with $w = 15mm$ ($TATCT_{w1}$) and 13mm ($TATCT_{w2}$) are 6.1% and 8.9% respectively lower than that with $w = 18mm$ (TATCT). It decreases with the decrease in the perimeter of cuts on the tape. The tape with smallest perimeter of cut therefore imparts lowest disturbance to the flow between the wall tube and edge of the tapes and correspondingly gives the lowest Nusselt number. The Nusselt number for the tape with $p = 27mm$ ($TATCT_{a1}$) and 18mm ($TATCT_{a1}$) are 2.5% and 7.9% respectively lower than that for the tape with $p = 34.26mm$ (TATCT). When the pitch (y) decreases from 54mm to 36mm the Nusselt number increases but decreases when the pitch increases from 54mm to 72mm. The tape with $y = 72mm$ ($TATCT_{y2}$) suffers a reduction in heat transfer rate of 3.4% of the tape with $y = 54mm$ but the twisted tape with $y = 36mm$ (TATCT) enhances heat transfer rate up to 2.1% over that of the tape with $y = 54mm$ ($TATCT_{y1}$).

C. Impacts of the Variations in the Tape Geometries on Friction Factor

It can be seen in Fig. 4 that as the tape width decreased from $w = 18mm$ (TATCT) to 15mm ($TATCT_{w1}$) and then to 13mm ($TATCT_{w1}$) the friction factor also decreased. The value of the friction factor when $w = 18mm$ decreases by 5.9% as compared with that when w = 15mm but decreases
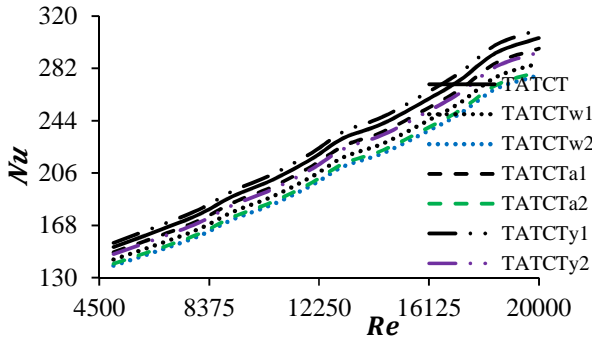
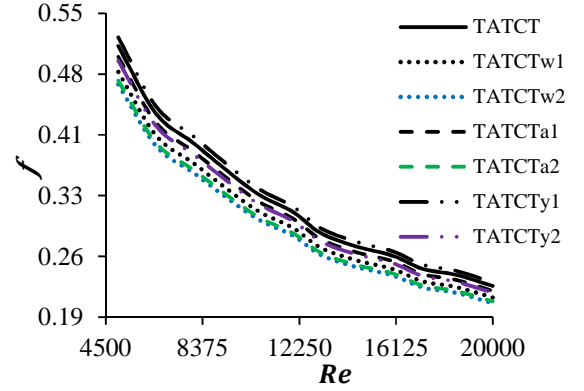Figure 3. Effect of variations in tape geometries of TATCT on Nusselt number vs. Reynolds number.

Figure 4. Effect of variations in tape geometries of TATCT on friction factor vs. Reynolds number.

by 8.6% when $w = 13mm$. The friction factor decreases as the perimeter of the cut decreases. This is because the additional dissipation of pressure of the fluid caused by the fluid disturbance due to the presence of cuts on the tapes resulted in an increase of interaction of the pressure force around a velocity boundary layer. The friction factors of the tape with $p = 27mm$ ($TATCT_{a1}$) and 18mm ($TATCT_{a2}$) are found to be lower than that of the tape with $p = 34.26mm$ (TATCT) by 2.3% and 7.5% respectively. It is increased with the pitch decreasing. The friction factors obtained with the tape with $y = 36mm$ ($TATCT_{y1}$) and 72mm ($TATCT_{y2}$) are 2.2% higher and 3.2% lower respectively than that obtained in the tape with $y = 54mm$ (TATCT).

D. Impacts of the Variations in the Tape Geometries on Thermal Performance Factor

The possibility of a twisted tape in promoting heat transfer is measured by thermal performance factor (η) [8, 10], which is expressed as

$$\eta = \frac{Nu/Nu_p}{(f/f_p)^{1/3}} \tag{13}$$

where Nu_p and f_p are the Nusselt number and friction factor respectively of plain tube.

As demonstrated in Fig. 5, the thermal performance factor increases as the tape width and perimeter of cuts on the tape increase but decreases as the pitch of the tape increases. The performances got from the tape with $w = 15mm$ ($TATCT_{w1}$) and 13mm ($TATCT_{w2}$) are 1.4% and 3.3% respectively lower than that of the tape with w = 18mm (TATCT). With the tape with $p = 27mm$ ($TATCT_{a1}$) and 18mm ($TATCT_{a2}$) the performance factors are 1.1% and 3.1% respectively lower than that with $p = 34.26mm$ (TATCT). The performance in $TATCT_{y1}$ ($y = 36mm$) is enhanced up to 1.1% over that of the tape with y = 54mm (TATCT) but with the tape with $y = 72mm$ (TATCTy2) the thermal performance diminished by 1.3% compared with that of the tape with y = 54mm.
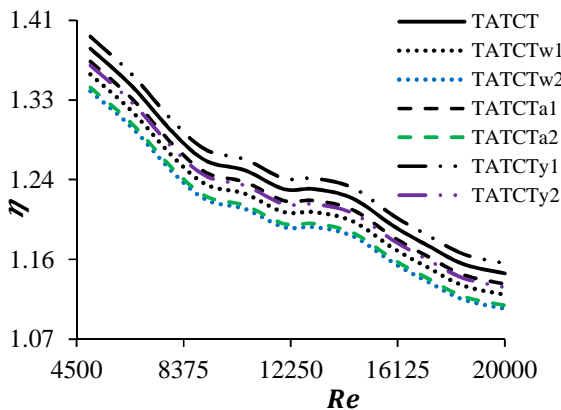
Figure 5. Effect of variations in tape geometries of TATCT on thermal performance factor vs. Reynolds number.

VIII. Conclusion

In this study, the effects of variation in tape insert on heat transfer and thermal performance characteristics in a tube flow were investigated. It was discovered that the heat transfer and thermal performance increasing the width and the size of the cuts on the tape is favourable to the heat transfer enhancement. Increasing the pitch of the tape resulted in the reduction in the performance of the system.

References

[1] A. Dewan, P. Mahanta, K. S. Raju and P. S. Kumar, "Review of passive heat transfer augmentation techniques," Proc. Instn Mech. Engrs, J. Power and Energy, vol. A218, pp. 509-527, 2004.

[2] R. M. Manglik and A. E. Bergles, "Heat transfer and pressure drop correlations for twisted -tape inserts in isothermal tubes: Part II - Transition and turbulent flows " Trans. ASME, J. Heat Transfer, vol. 115, pp. 890-896, 1993.

[3] H. J. Lane and P. J. Heggs, "Extended surface heat transfer—the dovetail fin," Appl. Therm. Eng., vol. 25, pp. 2555-2565, 2005.

[4] A. G. Patil, "Laminar flow heat transfer and pressure drop characteristics of power-law fluids inside tubes with varying width twisted tape inserts," Trans. ASME, J. Heat Transfer, vol. 122, pp. 143-149, 2000.

[5] S. K. Saha, A. Dutta and S. K. Dhal, "Friction and heat transfer characteristics of laminar swirl flow through a circular tube fitted with regularly spaced twisted-tape elements," Int. J. Heat and Mass Transfer, vol. 37, pp. 37-46, 2001.

[6] S. Eiamsa-Ard, C. Thianpong, P. Eiamsa-Ard and P. Promvonge, "Convective heat transfer in a circular tube with short-length twisted-tape insert," J. I Comm. Heat and Mass Transfer, vol. 36, pp. 365-371, 2009.

[7] P. Murugesan, K. Mayilsamy, S. Suresh and P. S. S. Srinivansan, "Heat transfer and pressure drop characteristics of turbulent flow in a tube fitted with trapezoidal-cut twisted tape insert," Int. J. of Acad. Res., vol. 1, pp. 123-128, 2009.

[8] P. Murugesan, K. Mayilsamy and S. Suresh, "Turbulent heat transfer and pressure drop in a tube fitted with square-cut twisted tape," Chinese J. Chem. Eng., vol. 18, pp. 609-617, 2010.

[9] Y. Chiu and J. Jang, "3D numerical and experimental analysis for thermal–hydraulic characteristics of air flow inside a circular tube with different tube inserts," Appl. Therm. Eng., vol. 29, pp. 250-258, 2009.

[10] T. Cui and M. Tian, "Three-dimensional numerical simulation of thermalhydraulic performance of a circular tube with edgefold-twisted-tape inserts," J. Hydro., vol. 22, pp. 662-670, Jul. 2010.

[11] S. W. Chang, Y. J. Jan and J. S. Liou, "Turbulent heat transfer and pressure drop in tube fitted with serrated twisted tape," Int. J. Therm. Sci., vol. 46, pp. 506-518, 2007.

[12] R. P. Benedict, Fundermentals of pipe flow, vol. New York: John Wiley, 1980.

[13] H. K. Versteeg and W. Malalasekera, An introduction to computational fluid dynamics- The finite volume method, 2nd ed., vol. England: Pearson, 2007.

[14] F. Inc. Fluent 6.3 user's guide, 2006.

[15] J. O. Hinze, Turbulence, vol. New York: McGraw-Hill Publishing Co, 1975.

[16] B. E. Launder and D. B. Spaldling, Lectures notes in mathematical models of turbulence, vol. London: Academic Press, 1972.

[17] Yakhot and S. A. Orszag, "Renormalization group analysis of turbulence I: Basic theory," J. of Scientific Computing, vol. 1, pp. 1-51, 1986

About Author s:

Taiwo O. Oni is a PhD student of Mechanical Engineering in the System, Power and Energy Research Division within the School of Engineering at the University of Glasgow, UK. His research areas include applied heat transfer, applied thermodynamics and applied fluid mechanics.

Manosh Paul (CEng MIMechE FHEA) is a Senior Lecturer in Thermofluids at Mechanical Engineering and a member of the Systems, Power & Energy Research Division within the School of Engineering of the University of Glasgow. He has been active in research in Thermofluids and CFD for the last 15 years. He is an author (or co-author) of over 70 refereed papers published in leading international journals and conference proceedings. He currently serves as a member of the editorial board of several international journals.